Deliverables D6.3.1 & 2
Piezoelectric response of PoC chips

PiezoMAT Deliverable D6.3.1 & D6.3.2 PiezoMAT – 2015-09-08 D6.3.1&2 *Piezoelectric response of PoC chips* *Option 2 (D6.3.1) & Option 3 (D6.3.2)*	
Contractual Delivery Date:	*M27 (D6.3.1) & M34 (D6.3.2)*
Actual Delivery Date:	06.10.2016 (*final version*)
Latest update:	
Author(s):	V. Lebedev, B. Christian, J. Volk, C. Sturm, N. Petkov, M. Seifikar, A. Graillot
Internal reviewers:	E. Saoutieff

RESTRICTED DISSEMINATION

REVISION HISTORY

Revision	Date	Description	Author
V1	M27	The first compilation	V. Lebedev
V2	…	Corrections by Elise	-
V3	…	Corrections by Janos	-
V4	06.10.2016	The final version	V. Lebedev

EXECUTIVE SUMMARY

Work package 6

Deliverable: T6.3.1&2: *Piezoelectric response of PoC chips Option 2 (D6.3.1) & Option 3 (D6.3.2)*

Lead partner: *Fraunhofer*

Estim. P×M: *11*

Delivery date: *M27(D6.3.1) & M34 (D6.3.2)*

The research reported in D6.3.1 & 2 has been carried out in Tasks “T6.3: Testing of PoC NW matrix prior to encapsulation” & “T6.4: Testing of PoC NW matrix following encapsulation” lead by FRAUNHOFER;

“T6.3: Testing of PoC NW matrix prior to encapsulation”

T6.3. started in M23 upon receiving of the first PoC2 (alternative version) samples from MTA and has been split in T6.3a (M23-M25) for PoC Option 2 and T6.3b (M29 to M31) for PoC Option 3 (fabricated by CEA), according to the new version of the PiezoMAT DOW;

PoC2 & 3 matrices with size of 8x8 and 10x10 NWs, respectively, were investigated prior the polymer encapsulation. FRAUNHOFER has been carried out the characterization of the charge/bias output signals from addressable piezo-pixels using analogue read-out lines upon calibrated-force nano-manipulation on the sensor surface (see the following section for details of characterization procedures). This task was aimed to provide insightful results for design and data processing optimization and for in-line characterization of final PoC & DEMO devices. The results delivered by these tasks serve as inputs for FEM model validation and optimization in WP3 (KTU) as well as feedback for optimization of DEMO chip design and fabrication route by CEA.

In T6.3, the same methodology has been applied as in task T6.1 for Option 1 samples. Here, the AFM-tip based measurements were performed on single NWs, which were assembled into a 2D inter-contacted matrix in order to verify the piezo-electromechanical parameters of the individual objects on patterned PoC2 & PoC3 chips prior to the polymer encapsulation step (SP). It was also planned that KTU and TYNDALL-UCC perform post-processing of the characterization results in order to analyze their consistency and adapt them for model optimization purposes.

“Task T6.4: Testing of PoC NW matrix following encapsulation”

T6.4 started in M25. It was split into T6.4a (M25- M27) and T6.4b (M32 to M34) focused on PoC Option 2 and Option 3, respectively. These tasks are devoted to detailed characterization of PoC 2 & 3 NW matrices fabricated by MTA & CEA, and encapsulated by the polymer matrix by SPECIFIC POLYMERS. The top ground electrode in Option 3 configuration has been fabricated either by deposition of Ag-

doped conductive polymer (SP) or by evaporation of Au top electrode onto pre-etched sensor surface (Fraunhofer). The program of the studies is identical to the T6.3.x tasks being carried out on PoC 2 & 3 chips containing 8x8 and 10x10 NW arrays, respectively. The main methodological difference is an applied force range. Compressive force applicable for AFM based technique is limited to ~ 1 µN due to the mechanical instability of the silicon cantilever. For encapsulated sensors such force magnitude is not enough for significant compression/bending deformation of the NWs embedded in a stiff polymer matrix. Therefore, in T6.4.x, the "macroscopic" force setup was employed, which is capable to apply forces up to 100 mN via a specially prepared tungsten mechanical prober mounted on nano-positioning XYZ-stage.

The scope of T6.3.1 & 2 is to demonstrate the sensing performance of PiezoMAT chip (proof-of-concept) in high resolution (up to 5.000 dpi). Similar to T6.1, the results obtained in T6.3.x serve as input data for FEM modelling in WP3 and array optimization for DEMO chip fabrication. In particular, the results of the piezo-electrical studies described in D6.3.x contribute to the fine tuning of the charge transport model developed by TYNDALL-UCC (T3.4) and KTU (T3.6) along with DEMO-chip development carried out by Morpho within T6.2: Circuitry fabrication for DEMO chips & Task T6.5: Testing of DEMO chips.

Content

1 Introduction

The PiezoMAT concept is to design a new technology of high-resolution fingerprint sensor based on a matrix of inter-connected piezoelectric nanowires (NWs). The direct consequence of integrating nano-objects rather than conventional microsystems is to diminish the size of individual pixels, which enables larger integration densities and thus higher spatial resolutions. This is the main technological objective of PiezoMAT.

In the case of the identified fingerprint sensor application, nano-objects are vertical piezoelectric nanowires (NWs), which act as nanoscopic force sensors distributed on the surface. The deformation applied on each ZnO NW generates a (piezo)-electrical potential within the NW. Collecting the charges induced by direct piezoelectric effect in each NW of a 2D matrix enables to reconstruct a 3D deformation field corresponding to the fingerprint (the third dimension is given by the incremental potential value as a function of the deformation rate). Hence charge collection on the surface of vertical ZnO NW is central to the piezoMAT concept.

The exact deformation applied onto a matrix of vertical NWs by a fingerprint is quite complex. Realistically, under finger pressure, high aspect-ratio NWs will undergo a deformation in the two directions of the plane (2D bending) rather than simply along their vertical axis (1D compression). PiezoMAT envisions collecting generated charges through three designs defined by charge collecting electrode pattern, named as Option 1, 2, and 3 (Fig 1.1). More details on the PiezoMAT sensor concept and detailed research program can be found in the Project's Description of Work and Project Part B documents located on www.piezomat.eu. In the focus of D6.3.1 & 2 are Option 2 & 3 PoC chips, which are very comprehensive from the technological point of view due to the involvement of multi-step processing including conventional lithography/etch technologies along with unique techniques and methodologies for selected NW growth and polymer encapsulation. Investigations on Option 2&3 samples deliver the detailed technical & scientific data towards various mechanisms of charge generation and electro-mechanical losses in ZnO NWs assembled into directly addressable, multi-pixel matrices. The data acquired in T6.3.x should support and improve the realistic "bent-NW" models, which are under development by KTU and Tyndall. For more details, see the deliverable **D3.3 Multi-physics model of a single, contacted, encapsulated NW**.

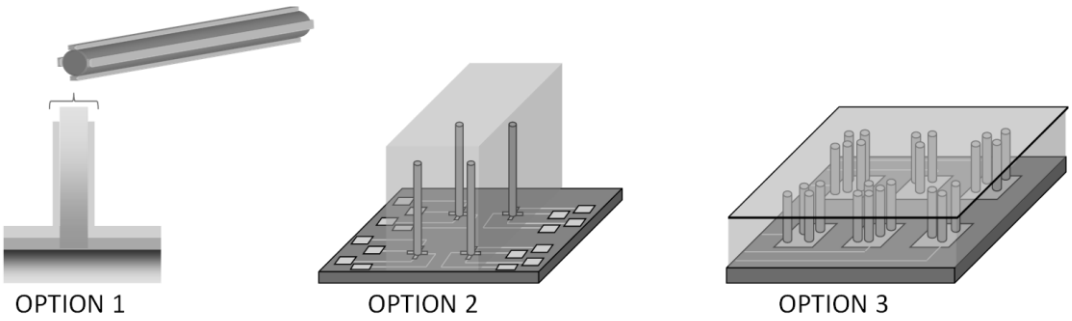

Fig. 1.1. *Electrode on NW configurations as defined in PiezoMAT DOW. (Option1) Single NW contacting by direct localised metal deposition; (option 2) Contacted NWs on chip with a 2-bottom contact configuration and an encapsulating polymer; (option 3) Contacted NWs on chip with a top-bottom contact configuration and an encapsulating polymer in the inter-electrode spacing.*

2 Layouts and fabrication of PoC chips

The general description of the technological layouts for both modifications of PoC chips can be found in the deliverable **D4.1 PoC layouts**. Please note, that due to the changes in the DOW, the layout of PoC option 2 chips (alternative, MTA version) have been changed drastically in order to speed up the fabrication process, while keeping the sensor lateral resolution of 5.000 dpi.

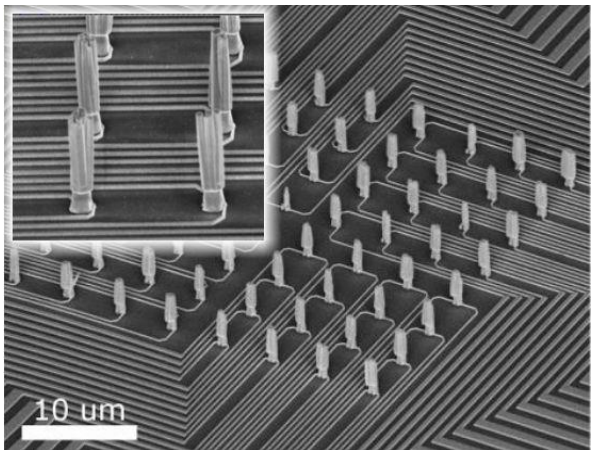

Fig. 2.1 *SEM images of PoC2A chips fabricated by optimized process on 3" Si wafer (MTA EK MFA).*

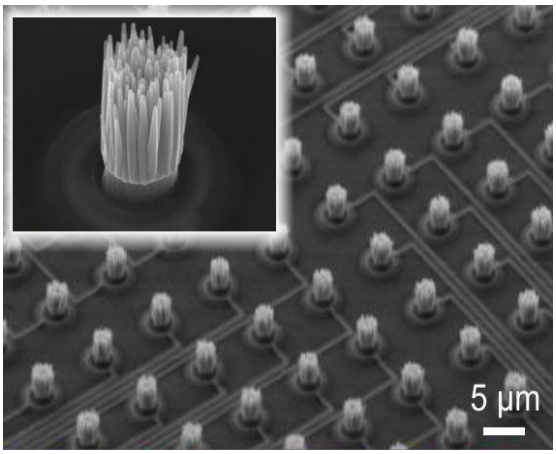

Fig. 2.2 *SEM images of non-encapsulated PoC3 chips fabricated by optimized process on 8" Si wafer (CEA Leti).*

2.1 PoC2 (alternative) 8×8NWs fabricated by MTA EK MFA

The actual PoC2 samples have been fabricated by MTA EK MFA using conventional processing methods combined with electron beam lithography. The PoC2 development had been started in CEA LETI, but was not finished due to fire accident in the clean room. Under these circumstances, an alternative version, PoC2A, was proposed and fabricated by MTA EK MFA in cooperation with ULEI and SP on 3" sapphire and Si wafers. The PoC2A chip has been equipped with two electrodes per pixel, instead of 4 electrode configuration foreseen for the original version. The main fabrication steps have been completed by MTA EK MFA through a 20 - step process flow including several nanolithography steps and the wet chemical growth of the NWs. The SEM observations confirmed that the 8x8 NW arrays are well oriented on the optimized Si chip, and each of them is properly accommodated to two metal contacts (see Fig. 2.1).

More technical details are given in deliverables PiezoMAT Deliverable 4.2.1 & 4.3.1, PoC chips processing and NW growth on PoC chips (Option2) - **D4.2.1 PoC chips** This report describes i) the difference between the original and the alternative layouts and technologies; ii) the challenges which have been emerged during the fabrication of PoC2; as well as iii) the main characteristics of the obtained chips which has been shipped to the partners for polymer encapsulation (SP), and further characterizations (MTA EK MFA, ULEI and Fraunhofer).

2.2 PoC3 10×10 NWs fabricated by CEA

The 10×10 pixel matrices have been fabricated according to the initial DOW by CEA Leti. The technical description of the fabrication process steps developed by CEA are described in the deliverable **D4.2.2 PoC chip processing - Option 3**, while the layout

of PoC3 chip is addressed in the deliverable **D4.1 PoC layouts**, and the choice of the materials are given in the **D3.2 Results of preliminary experimental studies**. In Fig. 2.2, SEM image of the active area from a "high-quality" PoC3 sample is shown demonstrating a multi-NW pixel configuration. This type of samples has been encapsulated by SP and later equipped with a top electrode (see Section 2.3) in order to complete the PoC sensor device.

2.3 Polymer encapsulation technology by Specific Polymers.

Encapsulations of NWs on PoC option 2 & 3 were performed using formulation and processes developed by SP and described in details in the **2nd Annual Report.** The details on chemical composition, spin-coating conditions and post processing of the polymer matrices can be found in the quarterly reports of the PiezoMAT consortium. Briefly, the spin-coating conditions were selected to reach desired thicknesses depending on the NWs length, which are different for PoC2 and PoC3 samples. In particular, in the case of PoC2, a layer thickness equal to NW length + 2 µm was targeted in accordance to the latest KTU model.

The example for encapsulated PoC3 pixel is shown in SEM micrograph (Fig. 2.3). From SEM observation it is not obvious if the tip of the NWs is free of polymer. Moreover, it was found that the encapsulating polymer degrades under electron beam which was utilized as an alternative etching-back process. Here, the polymer thickness is much smaller comparing to the PoC2 encapsulation due to the necessity of the top ground electrode uniting upper sides of the NWs in the whole matrix. Therefore, the top electrode is deposited on top of the insulating polymer matrix being in electrical contact with NWs. To free the upper parts of the NWs from the polymer, the partial etching of the insulating polymer matrix by means of oxygen plasma processing and direct electron beam writing have been employed in Fraunhofer and MTA EK MFA.

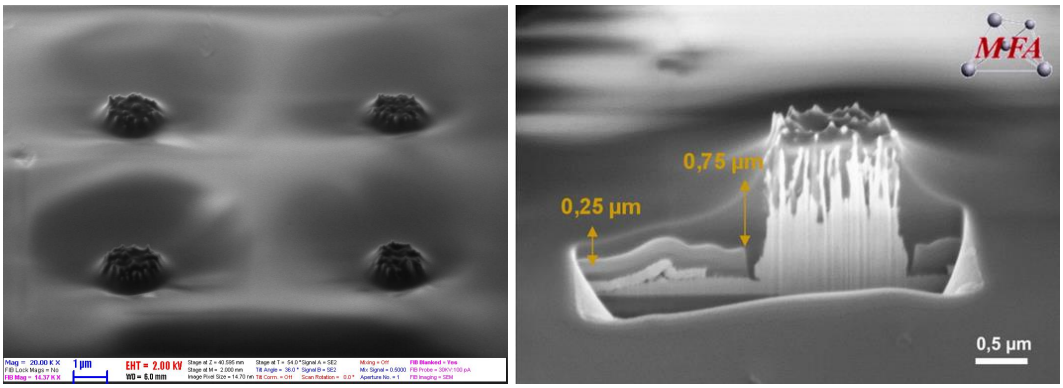

Fig. 2.3 *Encapsulated ZnO NW bunches on PoC3 (P07_7): before (a) and after (b) FIB cut on.*

.

2.4 Etching back of the polymer encapsulation (PoC3)

For the PoC3 chips, various strategies have been developed by the PiezoMAT consortium in order to fabricate a suitable configuration for the top sensor electrode. Main concepts propose that the non-conductive polymer layer (matrix) with thickness slightly lower than the NWs length should be fabricated first. To establish an electrical contact to upper end of the NWs, the polymer is partly etched in the oxygen plasma (see Fig. 2.4ab). Due to the very thin polymer layer conditions outside the active area

($d_{polymer}$~0.25 µm, see Fig. 2.3), in order to prevent the short cuts in the electrical interconnection, the amount of insulating polymer to be etched is very limited. Therefore, as shown in Fig. 2.4a, it was not technically feasible to remove polymer completely from the pixel top. Consequently, the NWs located in the middle of the pixel bunch remain covered by insulating layer.

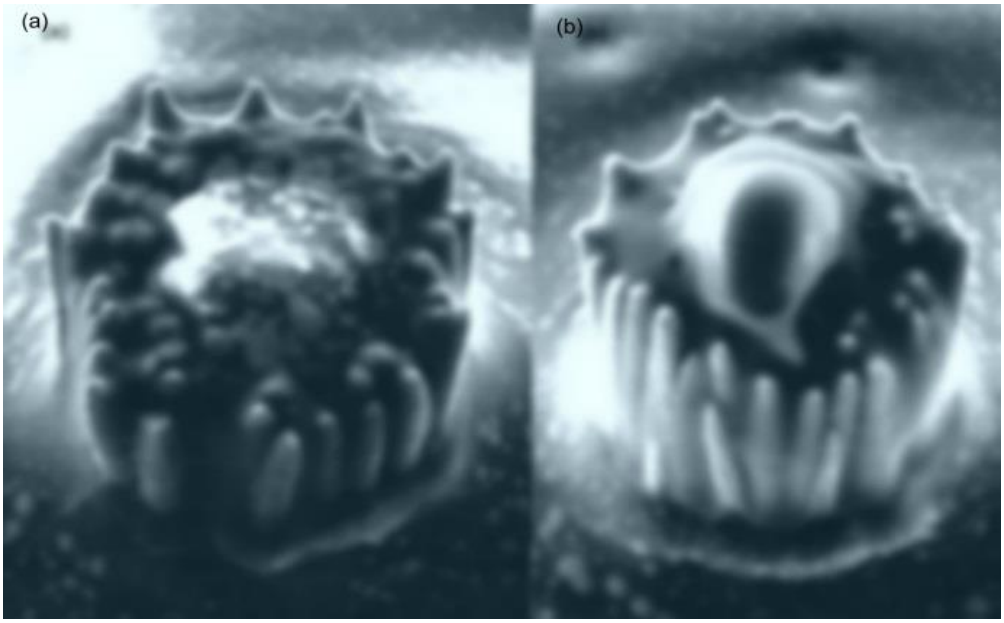

Fig. 2.4 *SEM micrographs of (a) encapsulated PoC3 pixel processed in oxygen plasma at 600 W during 180 seconds (Fraunhofer); (b) "as-deposited" encapsulation prior to the etching (SP & MTA EK MFA);*

Beside oxygen plasma etching MFA has elaborated an alternative technique for localized polymer etching using electron beam. The process is very similar to standard e-beam lithography but here the encapsulating polymer is directly etched by electron beam. Before processing the actual sample a dose optimization had been carried out. As shown in Fig. 2.5 the depth of the rectangular depression is increasing with the electron dose. For further details please refer to **QR10**.

Selecting optimal dose, circular windows were opened by electron beam above the ZnO NW pixels on the PoC3 sample (P07_7). In order to verify the etching-back process conductive AFM technique using a Pt probe tip was used before top contact deposition. In this experiment we did not aim to measure I-V curves and define resistance rather recording a map to differentiate the conductive (ZnO NW out of the polymer) and non-conductive (polymer covered) regions. As shown in Fig. 2.6 we obtained conduction in a few tip positions. Since these conduction spots are mainly localized near to the edge of the bunch we think that the tip of the conductive AFM probe was worn off and conduction could occurred only when its side attached the NW. Nevertheless, it confirms that a limited portion of the NWs pierce the polymer, so we sent back the sample to Specific Polymers for top contact deposition.

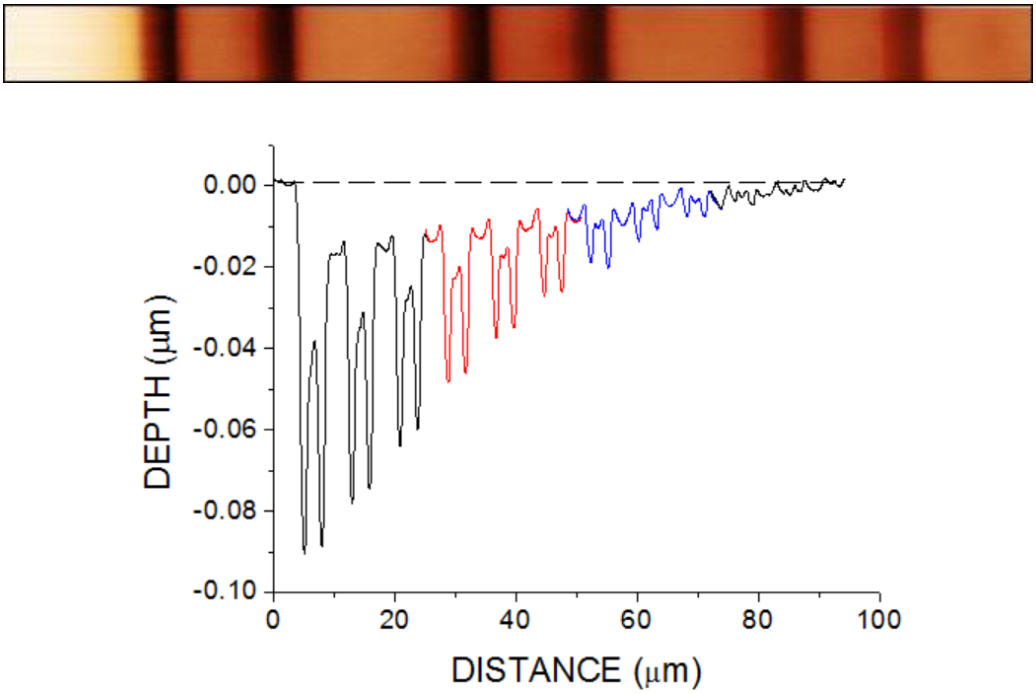

Fig. 2.5 *AFM tapping image on the first six dose test rectangles (a) and a stiched line cut across the whole series of dose stripes (b). As expected etching depth scales with the dose.*

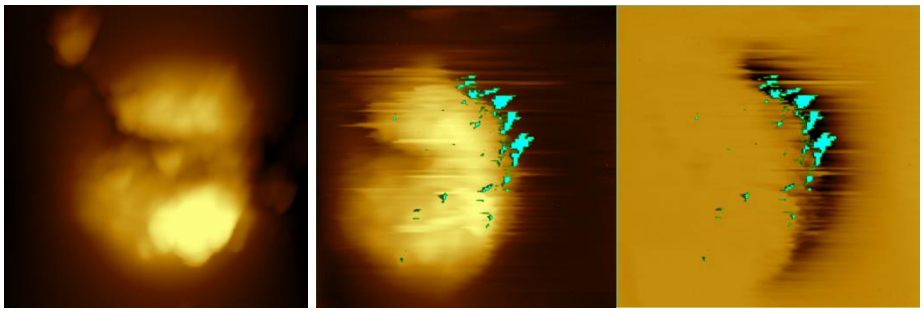

Fig. 2.6 *AFM images on encapsulated PoC3 (P07_7) aftrer e-beam localized etching recorded in tapping mode (a) and in contact mode showing normal (b) and lateral (c) force signal maps. The obtained conduction sites (cyan spots in (b) and (c)) were found mainly around the inverted peaks in the later force signal.*

In summary, oxygen plasma is an economic process for etching back the encapsulated PoC3 devices. However, the accurate setting of the etching time is challenging mainly because of the low thickness of the polymer. As an alternative process, MFA developed a localized etching using e-beam lithography system which was verified by conductive AFM. This technique is more expensive and sophisticated than oxygen plasma etching. The consortium has decided to use both techniques in parallel (oxygen plasma at Fraunhofer and e-beam at MFA) in the project to minimize the risk.

2.5 Fabrication of the top electrodes (PoC3)

After the plasma processing, the active area of the chips has been covered with different electrode material. First, a 100 nm thick gold layer was fabricated by conventional evaporation in Fraunhofer (Fig. 2.7a). The gold shows an excellent adhesion to the polymer surface remaining flat, appropriately flexible and highly conductive in 100 nm thickness range. The main drawbacks of this approach are related to the difference in the mechanical properties of the polymer and metal layers leading to the crack formation during the mechanical probing of the sensor. This effect is illustrated in Fig. 2.7d, where the cracks in the Au electrode were observed after multiply mechanical probing of PoC3 sensor.

The Ag nano-particles suspended in the liquid have been used as an alternative option to the solid metal electrode. The nano-droplet of Ag-suspension has been placed on top of the active area and dried out at the ambient conditions. The resulting layer is highly conductive consisting of Ag nano-particles weekly linked to each other (Fig. 2.7b). This method allows for formation of highly flexible and conductive electrode. However, the thickness of the layer is hardly controllable on the sub-µm scale.

The second option – the use of a silver based polymeric hybrid material as a top electrode – is the most prospective option being developed by SPECIFIC POLYMERS (Fig. 2.7c). The conductivity of silver based polymeric hybrid layers was confirmed to be very high, indeed sheet resistance of corresponding samples were measured by MTA-MFA ranging from 1 to 60 Ω/sq. Nevertheless, SEM and interferometry images

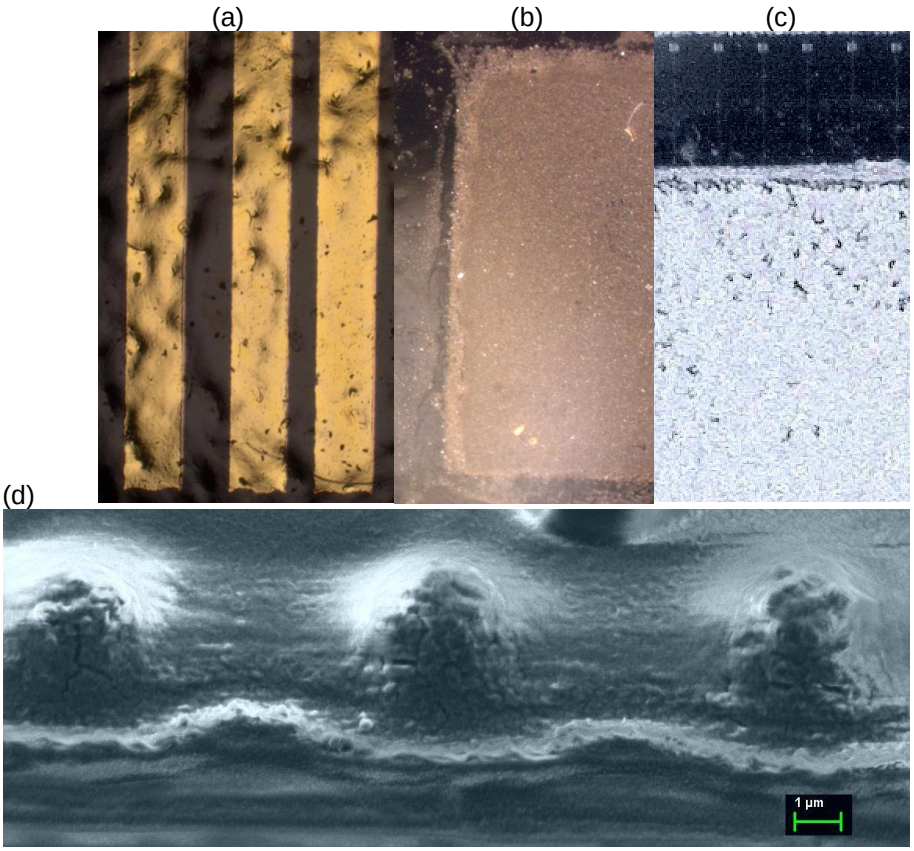

Fig. 2.7 *Different types of top electrodes fabricated on top of the active area of PoC3 sensor: (a) 100 nm Au layer by Knudsen evaporation (Fraunhofer); (b) silver nano-particle layer (Fraunhofer); and (c) hybrid silver/polymer layer (SP). (d) SEM image of the Au electrode surface after multiply circles of mechanical probing.*

also reveal that surface of such layers are rough and inhomogeneous and thus can imply some issues when used as top electrode for option 3 PoC chips. At the current stage of the project, all three types of top electrodes are still under evaluation, being tested during electromechanical experiments at Fraunhofer.

3 Experimental setups and methodology for piezo- and electrical studies

3.1 Printed circuited boards for PoC2 & 3 chips

The construction of "low-profile" printed circuit boards (PCB) and "low-noise" signal interfaces for the force-load multi-channel electrical characterization using DDC264EVM ADCs and KEITHLEY 2612A Source-Meters (on PoC2 & 3) has been completed and tested (see Fig. 3.1 and QR10-11 for more details). New PCB has been tested in both, AFM and macro-force environments. The main technical issue, a low operational signal to noise ratio (SNR), however, remains a challenge, especially, for multi-channel measurements using DDC264EVM.

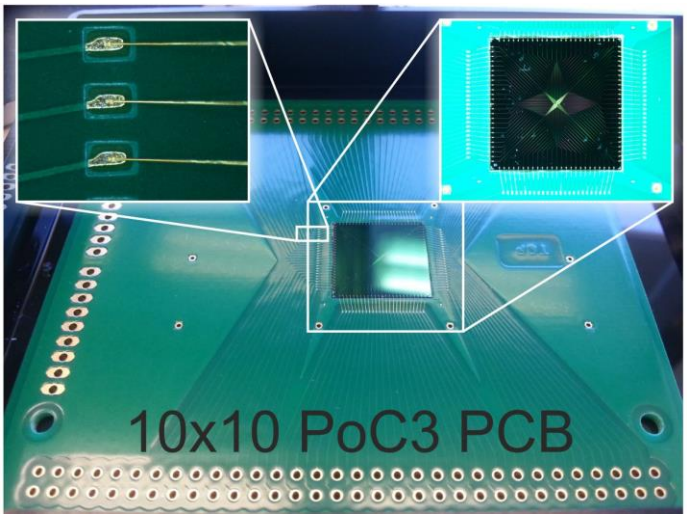

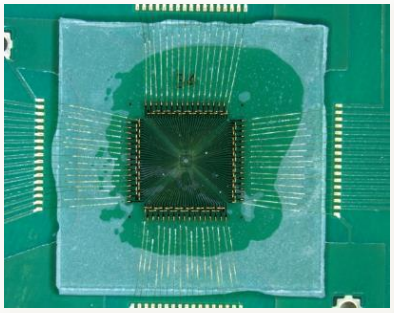

Fig. 3.1 *Optical micrographs of the solidly mounted and wire-bonded PoC3 (left) and PoC2 (right) chips on the low-profile PCBs prepared for the low-noise electrical measurements. (Fraunhofer);*

3.2 Wire bonding technologies and analog interfaces

The main challenge recognized during the studies of PoC2 & PoC3 piezo-response is a low operational signal-to-noise ratio (SNR), which is a critical issue for the characteristic pA-level of generated signals. In order to improve SNR, 2-level PCB designs along with electrically screened multi-core cables were employed for the measurements.

The analog interfaces were organized in the following way:

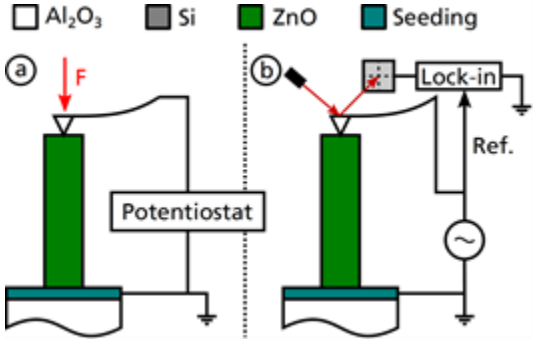

Fig. 3.2 *Schematic representation of the AFM based measurement techniques: a) force-response; and b) piezoelectric coefficient measurement configurations.*

1) signal from single standing, not encapsulated NWs have been measured by applying mechanical force onto the individual NW's top-end via conducting AFM tip (compressing); the generated signal has been recorded by digitalizing the analog signal (current) measured between top and bottom NW contacts using either potentiostat or electrometer over the time; for more details see the next section.
2) the multi-channel signal from encapsulated NW arrays have been measured by means of several 2-channel Keithley 2612A source-meter devices. In this case the Cu-Be needle DC-probes have been employed. The measurements with DDC264EVM ADC card have been carried out only on the wire bonded probes. The PoC2 chips having large margins surrounding the chip area were bonded using manual ball-wedge bonder, while PoC3 samples were bonded using automatic (programmed) regime (see Fig. 3.1 right&left, respectively).

By using wire-bonding techniques combined with a proper selection of analog cable properties, the optimal conditions for detection of pA level signals have been met. This allowed for the effective recognition and recording of the signals at low SNR without using special measurement methods (e.g. lock-in technique) or post-treatment of the results (e.g. FFT filtering).

3.3 AFM based setup at Fraunhofer: construction and experimental data treatment

Two AFM setups for investigation of i) force-response and ii) piezo-electric properties of single standing NWs have been constructed. These two setup's configurations are schematically described in Fig 3.2. In the current report, only a short introduction to the developed methods is provided. See Annual Reports 1&2 for more technical details.

In both cases, a *tapping* mode AFM was employed to localize the nanostructure of interest. In the force-response mode, the force is applied to NW top by lifting down the AFM tip to the prior determined z-position. The bending of the cantilever is proportional to the force and correlates to the deflection of the laser spot at the photo diode. By setting a certain voltage set-point at the photo diode, the z-axis piezo driver goes down until a certain force is reached and the potentiostat measures the released charge in form of a current flow.

To determine the piezoelectric coefficient (effective value of d_{33}) of the localized NW, the nanowire is contacted permanently via conducting AFM tip and excited by means of an external AC voltage generator. The output of the photodiode is then measured by a lock-in amplifier using the excitation frequency as a reference. For the calibration of the setup, in order to determine d_{33} (effective value) of ZnO NWs precisely, the cantilever sensitivity and reference piezo-response of AlN micro-pillars (predefined d_{33} = -5.8 pm/V) were measured.

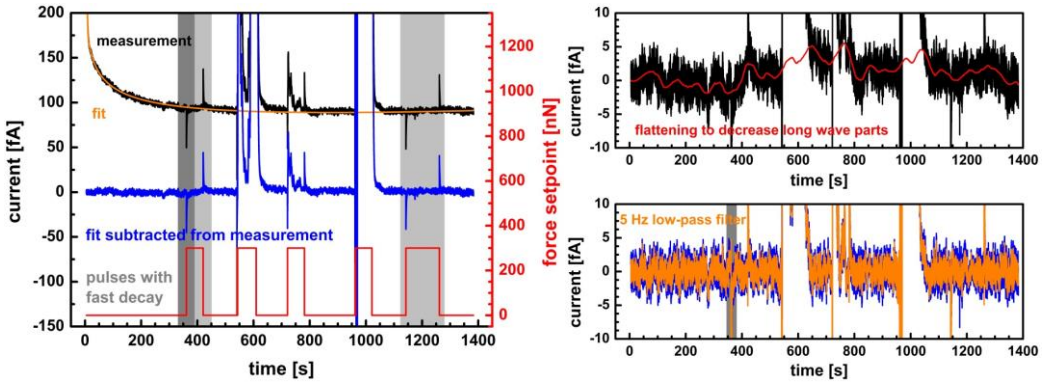

Fig. 3.3 *Post-treatment of the raw experimental data obtained by the force-response measurements applied to decrease the noise and analyse force response peaks.*

Besides of the calibration procedures performed prior to the measurements, the extensive post-treatment of the obtained data has been also carried out (see Fig 3.3). In particular, the signal measured by potentiostat contains an electrical offset appearing at the start of each measurement, which magnitude decreases exponentially over the time. This offset is removed by exponential fitting of the raw data. In addition, to improve SNR, FFT filtering as well as polynomial fits have been employed. Thus, the resulting plot only shows the force-response peaks correlating to the applied force, which is proportional to the voltage set-point at the QPD (the cantilever deflection), and this data was used for the piezo-response analyses.

3.4 AFM based setup at MTA EK MFA for NW bending tests

AFM bending tests of PoC2 were carried out in MFA by simultaneous monitoring of lateral force and electrical signals. At first the later force signal of the AFM tip was calibrated. Instead of the most commonly used by rather inaccurate geometrical method we used diamagnetic levitation technique (Fig. 3.4a-d). Here, a levitated pyrolytic graphite sheet was used as a lateral spring gauge as proposed by Li et al. (Rev. Sci. Instrum. 77, 065105 (2006)). Before starting the AFM test the PoC2 chip to be tested were glued on a small size chip holder PCB. 8 selected NW circuits out of the 64 were wire-bonded at once and tested by source measure unit. After mounting the PCB on our AFM (Smart SPM 1010, AIST NT) and connecting source-drain into the conductive unit of the AFM, NWs were localized by tapping mode. It was followed by a slow descending with continuous line scan of the tip in contact mode without any feedback. As soon as a lateral force signal was detected the tip approach was stopped and a finely controlled bending was carried out from the side of the NW pixel by changing the lateral x position of the sample. Each bending tests were started by taking an I-V curve in unloaded condition. Several time-domain and lateral force dependent measurements were carried out at various bias voltages on both bare and polymer encapsulated samples. Since both the lateral mapping and current signal were done by the AFM instrument the obtained results and maps could be easily compared with the same controller software (Fig. 3.4, right panel). Altogether more than 10 sapphire and Si based chips and about 40 NWs were tested both in bare and in polymer encapsulated conditions.

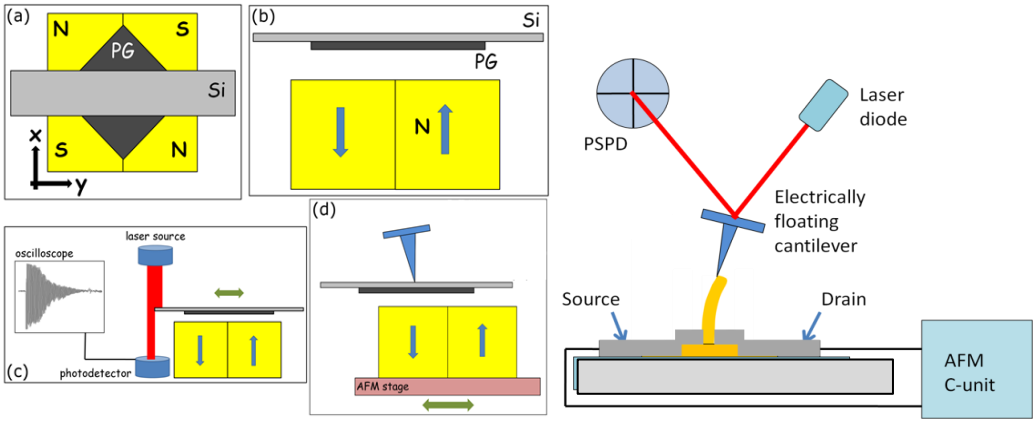

Fig. 3.4 Calibration of the *lateral force signal of the cantilever using diamagnetic levitation method (a-d) and the schematics of the NW bending setup of MFA (right panel). Electrical properties and lateral force signals were in-situ monitored using the conductive unit of the SmartSPM 1010.*

3.5 "Macro-force" setup with nano-mechanical positioning

The majority of the piezo-characterization experiments in Fraunhofer have been carried out by means of a macro-prober with nano-mechanical positioning using a multi-needle-probe configuration. The range for the applied forces does not exceed 100 mN. The time-domain electrical response from NW matrix has been recorded by multiply KEITHLEY source-meter devices (4x type 2612A), and the acquired signal has been analyzed by LabView-based software written for this particular measurement configuration.

As shown in Fig. 3.5, the developed "macro-force" measurement system has been composed of the following components:

- mechanical probe: rounded W-needle located on the nano-positiometer (XYZ-range 100 µm, precision +-1 nm), which is controlled via PC to provide periodic load onto the samples surface;
- the mechanical probe position is controlled visually through microscope cameras delivering top- and side-view live images to the PC;
- PoCx sample is mounted on the force sensor; however it is not sensitive enough to prevent the damage of the NWs during the first contact; therefore, the visual and electrical signal controls were employed to adjust the system for the "force-load" tests.

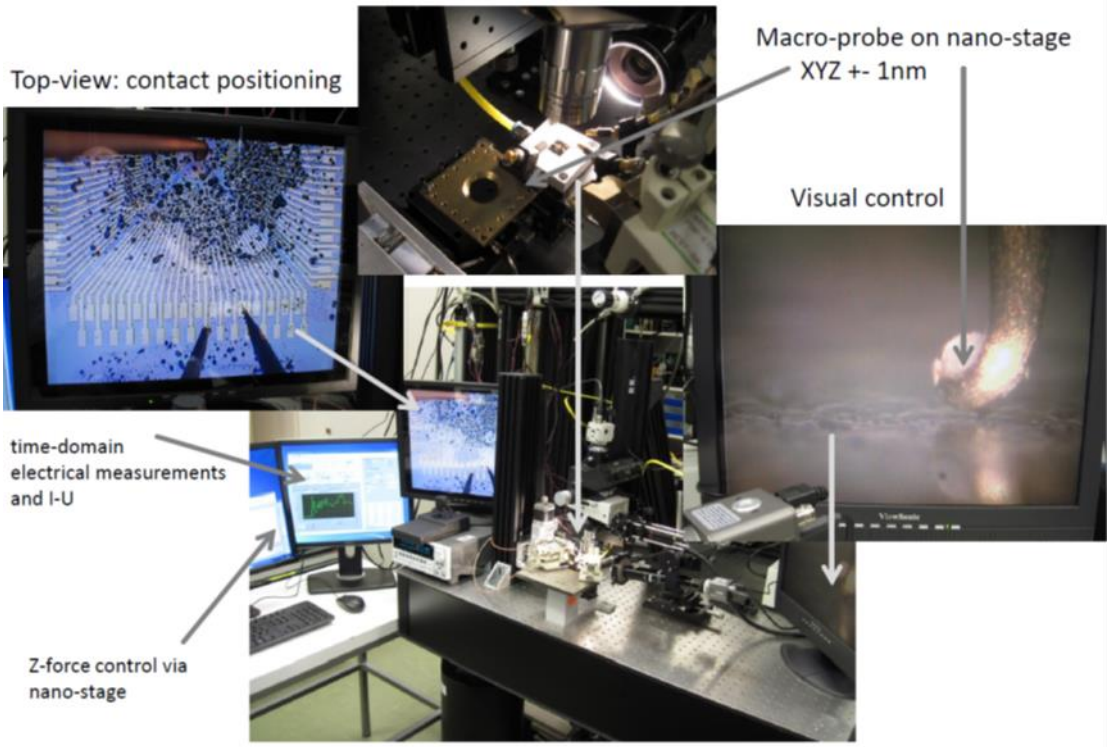

- not-bonded and mounted/bonded samples are connected via CuBe needle-probes mounted on the micro-manipulators (for four independent channels at the moment); the bonded probes are connected either through the 64-lines interface cable to the DDC264EVM ADC card or through shield coaxial cables to the Keithley 2612A source meters;
- measurement equipment: four Keithley 2612A dual-channel source-meters with sensitivity up to 5 pA;
- the applied voltages have been varied from 0 (preferable "piezo-generator" regime) to 20 V depending on the individual resistance of the pixel/NW;

4 Studies of not encapsulated (NE) sensors using AFM-based technique

4.1 Electro-mechanical characterization of individual NWs

Force-response and piezo-electric measurements (see description in Section 3.3) have been carried out on the individual ZnO NW pixels, in order to study the force sensitivity of piezo-electrical NWs in the different ranges of the applied force. For this purpose, the obtained peak response has been analyzed in time-domain, in order to evaluate the electro-mechanical interaction between the AFM tip and NW. The results of these analyses are depicted in Fig.4.1.

In Fig.4.1a, one can see that negative current peaks ("compression") show a weak dependence to the applied forces, while all positive peaks ("release") are nearly equal in magnitude. The value of the net generated charge (the orange plot) is following the current dependence. The force dependence has much more pronounced character, however, if the first derivative of the current over the time is analyzed (the red curve). It reflects, in particular, the increase in the velocity of AFM-tip approaching the NW. In addition, comparing the "compress" and

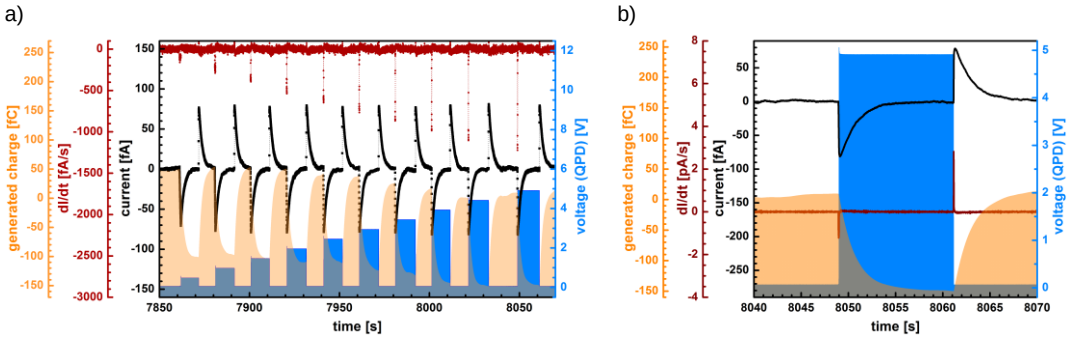

Fig. 4.1: *Force-response measurement carried out on single NW: (a) multi-circle force-variable measurements; (b) detailed "compress/release" analyses of the force response of the NW.*

"release" signal magnitudes (Fig. 4.1b), one can see that the corresponding peak values in the dI/dt curve is quite different. This interaction can be described by Lennard-Jones model (*LENNARD-JONES-Potential*[1]): the cantilever tip pressing the NW surface is reflected by the atomic repulsive force, while during the release, the adhesion force acts between tip and NW making release process slower. Also, it is clearly shown that the generated charge is comparable for press and release, although the slope of the force-response peak is different.

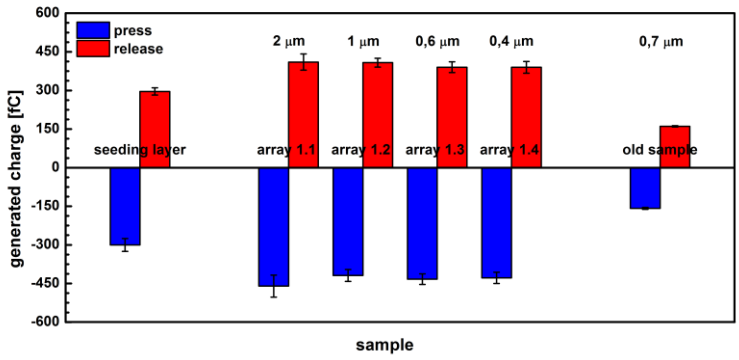

Fig. 4.2: *Comparison chart of the generated charge measured on GZO seed layer and NWs of different diameter upon applying compressive force (the blue bars) followed by NW release (the red bars).*

For further analyses of the force-response behavior, the individual NWs with different diameters have been investigated. All measurements on these NWs were performed using the same AFM cantilever in order to keep the measurement results comparable. On every NW under test, photo-diode voltage set-point of 5 V has been applied 10 times and the press- and release- responses have been measured (Fig. 4.2). One can see that the calculated charges demonstrate an expected weak dependence on the NW diameter – the NWs having larger diameter (larger volume) generate a higher charge level. In addition, comparing the results obtained on the first (old) and second generation samples, one can conclude that the NW quality (electro-mechanical properties) has been drastically improved due to the constant optimization of the NW fabrication technology.

[1] *Lennard-Jones, J. E. (1924), "On the Determination of Molecular Fields", Proc. R. Soc. Lond. A, **106** (738): 463–477.*

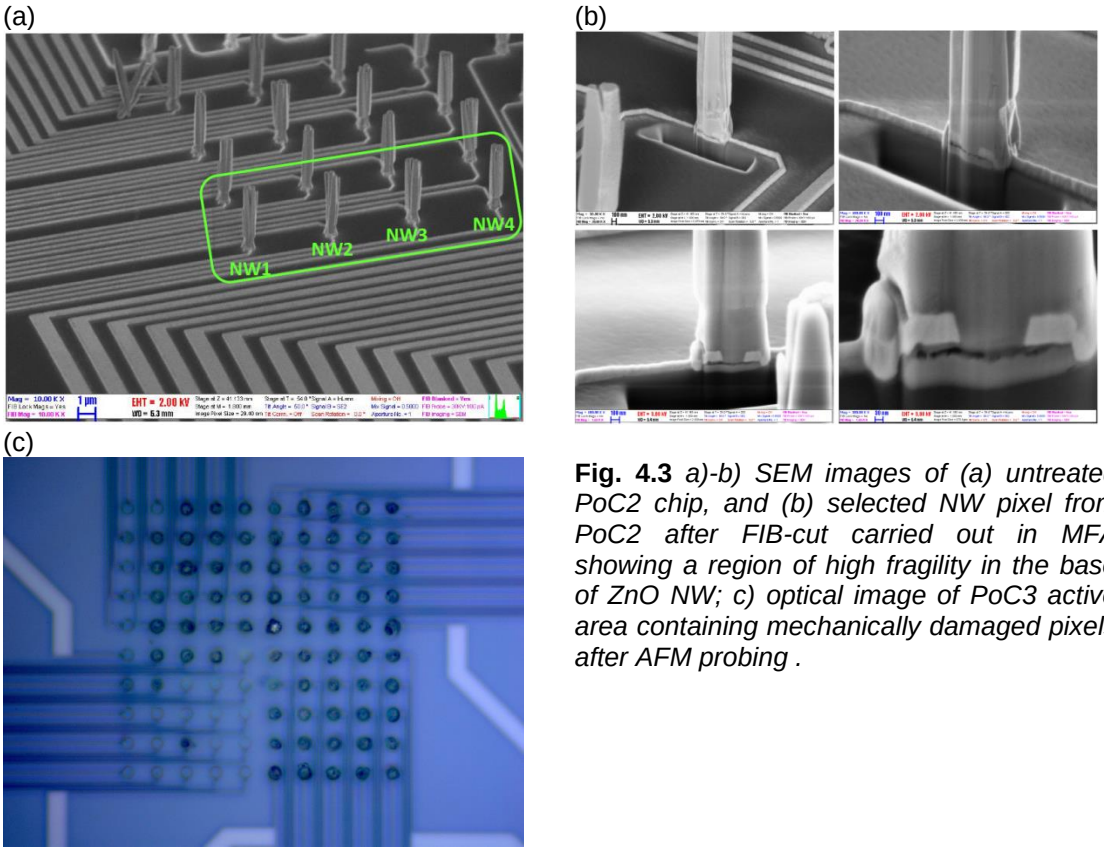

Fig. 4.3 *a)-b) SEM images of (a) untreated PoC2 chip, and (b) selected NW pixel from PoC2 after FIB-cut carried out in MFA showing a region of high fragility in the base of ZnO NW; c) optical image of PoC3 active area containing mechanically damaged pixels after AFM probing .*

4.2 Electro-mechanical characterization of NE-PoC2&3 chips

Free-standing (not encapsulated) NWs from both types of PoC device have been tested by AFM conducting tip (Pt coated Si cantilever). Usually, in this configuration, the maximum applied mechanical force is limited by the ~ 1 μN level due to a AFM-cantilever breakability. However, for both tested options of PoC chips, the fragility of NWs did not allow to reach the load force required to generate a recordable signal. In the following, the examples are given for PoC2 samples, however, the experimental observations are quite similar for both Option 2 and 3 NWs fabricated on Si substrates.

In the case of PoC2, all the attempts to increase the force load over 100 nN result in breaking the NW so as it cannot sustain a lateral component of the force arising due to the bending of the cantilever. The possible reason for this phenomenon is illustrated by SEM images taken in MFA on untreated and FIB-cuted NWs from PoC2 chip (see Fig. 4.3). The region at the base of NW is showing obviously a macro structural defect (plane) arising between NW bulk and ZnO seed layer, presumably during the nucleation, which results in a very high mechanical fragility of the NW pixel.

4.3 Summary of the studies

Due to the lack of mechanical stability, it was not possible to probe the non-encapsulated PoC2 & 3 chips within the force range appropriate for the detecting reasonable level of generated electrical signal. Due technology-related delays in PCB design & construction along with PoC2&3 sample deliveries, it was decided currently to concentrate our efforts onto polymer-encapsulated NW samples, where the polymer matrix guarantees an additional stiffness for embedded NW

pixels allowing for a much higher magnitude of the mechanical force to be applied.

5 Electro-mechanical characterization of encapsulated PoC sensors

5.1 Electro-mechanical characterization of PoC2 chips using macro-probing

The initial tests on a macro-force probing of encapsulated PoC2 samples have been performed at MTA EK MFA by covering an active area of PoC2 chip using a 200 µm thick PDMS pasted on the top of the nanowires using silicone monomers. The cyclic force-load experiments were performed by means of applying hemispherical probe tip of manual force-gauge to the disk surface and recording the generated voltage signal by a National Instrument data acquisition card (see Fig. 5.1).

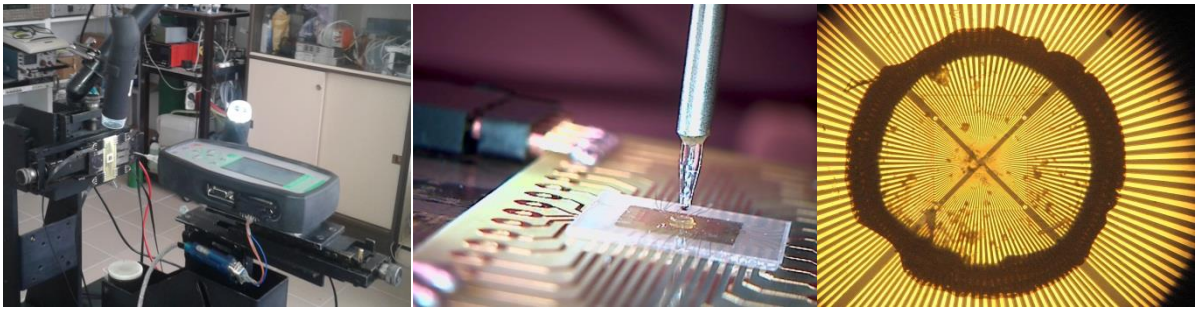

Fig. 5.1 *a) Optical image of a PoC2 chip probing configuration at MFA: force gauge mounted on a goniometer (a), tapered glass probe in unloaded position (b), and PoC2 chip (W3356) covered by a home-made PDMS disk (c).*

These first experiments demonstrated that PoC2 chip delivers a reproducible electrical signal in low-force range (~20 mN). The increasing force 25 mN, however, leads to the unrepairable damages of the pixel structures, which is obviously seen in the time range 200-350 s in the plot shown in Fig. 5.2.

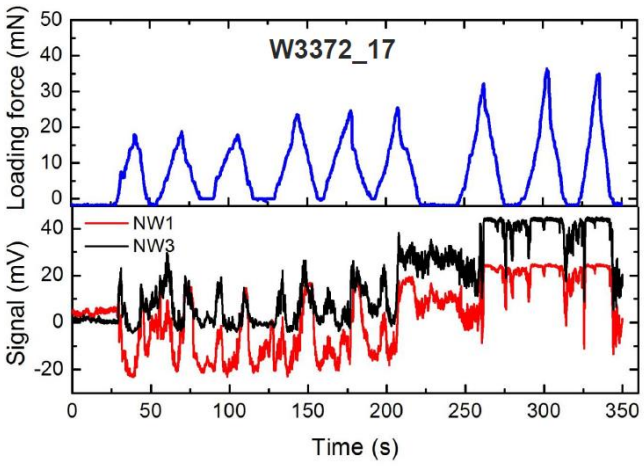

Fig. 5.2 *NW multi-pixel electro-mechanical response recorded on PDMS-disk covered PoC2 chip upon mechanical impact from the force-sensor tip.*

5.2 Characterization of PoC2 chips using nano-positioning technique (Fraunhofer)

Two types of encapsulated PoC2 chips fabricated by MTA EK MFA & SP have been tested in Fraunhofer – fabricated on Si and sapphire substrates. The crystal quality of ZnO NWs grown on silicon and sapphire substrates is quite different: NWs grown on patterned sapphire chips are single crystalline with well-defined hexagonal cross-section shape, while NWs grown on silicon are assemblies of NWs with a small diameter having common base and the same c-axis orientation.

The differences in crystal quality define also the electrical behavior of the piezo-pixels in the great extent. No electrical response has been detected on PoC2 samples (totally 4 samples have been tested) grown on Si chips if no external voltages have been applied to the two contacts located at the base of the NW (see Fig. 4.1a for the typical sample SEM image). The reproducible electrical response upon the force load for two parallel channels has been observed at 20 V applied bias. However, the dynamics of the response seems not fitting the typical NW behavior, which usually follows an exponential decay in the signal after the first contact and after the interruption of the connection (see **QR10** and **AR2** reports for details). It looks more like that the mechanical probe acts as a shunt for the pixel decreasing the total resistance with no changes in capacitance.

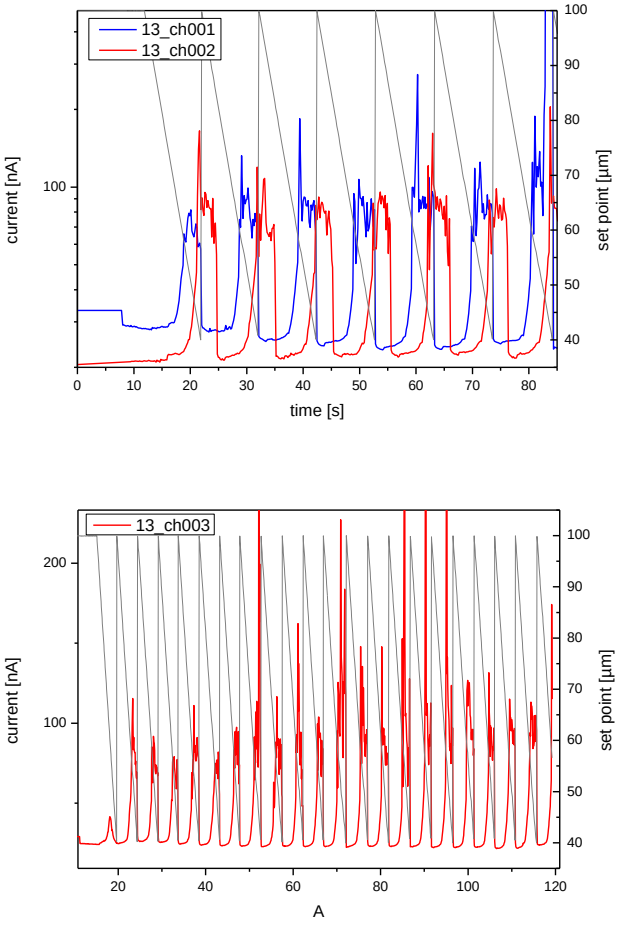

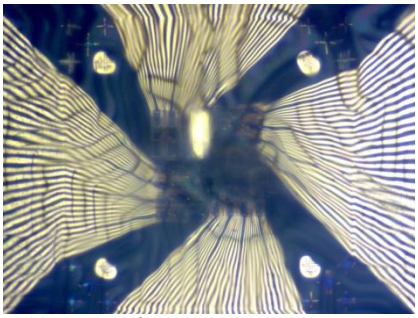

W3372-13 active area

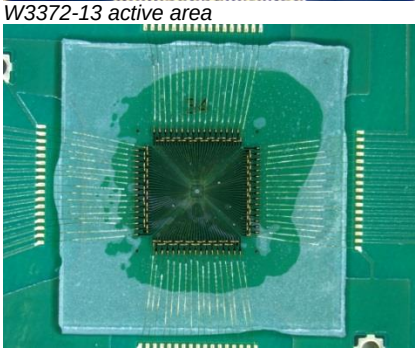

PoC2 on sapphire wire-bonded on PCB;

Fig. 5.3 *Electrical response of PoC2 chip on Si at 20V applied bias upon compressive mechanical impact using a "macro-force" setup at Fraunhofer IAF: a detailed two-channel response (top-left) and a long term test (bottom-left) of a single channel.*

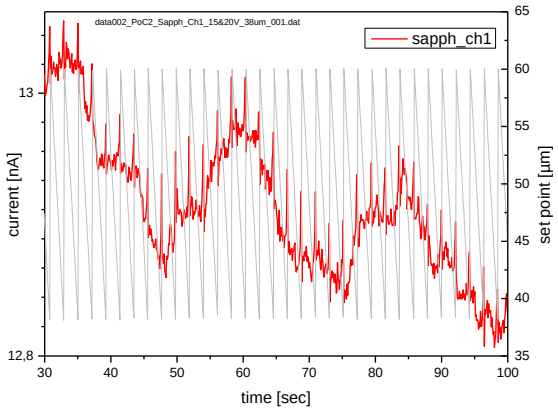

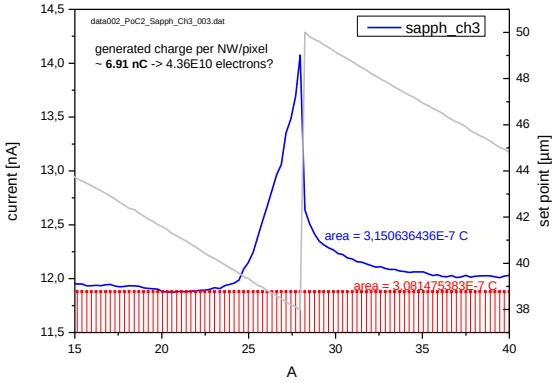

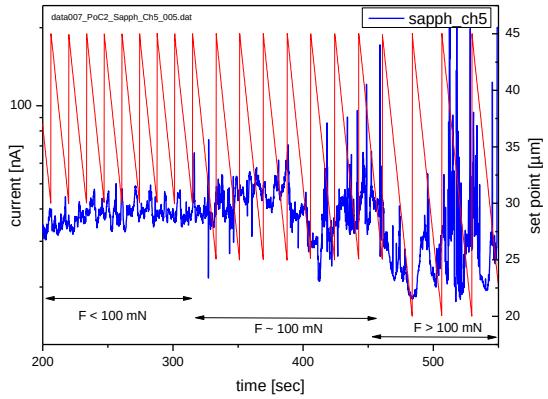

Fig. 5.4 *Electrical response of PoC2 chip on sapphire upon cyclic compressive mechanical impact using a "macro-force" setup at Fraunhofer IAF: a) a long term test of a single channel with an electronic drift; b) detailed analysis of the time-domain response; and c) force depended electro-mechanical response of NW pixel.*

Several mechanically and electrically stable NW pixels have been used for a long-term cyclic test using force variation conditions. The results shown in Fig. 5.3 (left-bottom) support the first observations that mechanical contact with the samples just changes the Ohmic resistance of the pixel with no NW "piezo-tronic" action, therefore no force-dependencies have been observed at the current stage of studies. The magnitude of the measured signal shows no stability in time.

Therefore, as it can be summarized from the measurements on 3 sensor chips, functionality of PoC2 on Si cannot be described as either "piezo" or "piezo-tronic". At the moment, all sensors deliver binary information – "contact-non-contact", and no obvious force dependence of the signal (which can be precisely quantified) has been recorded for any channel. The main reason for this behavior can be observed macro-structural defects and consequent fragility of NW pixel structure. These experiments will be continued in Fraunhofer and in MTA EK MFA upon receiving new NW structures with a less fragile texture.

The PoC2 structures on sapphire substrates have been fabricated as a reference in order to compare ZnO NWs of high and reproducible quality with bundle-like structures typically grown on Si. No principal differences, however, have been detected by "macro-force" measurements carried out on these two types of PoC2 chip. Despite of the fact that a reproducible electrical response upon a force load has been detected at 10 V bias, an electronic drift in a signal level is enormous (see Fig. 5.4. At 20 V DC bias, the NW is quickly degrading.

For the technical purpose, it can be calculated that the mechanical contact of the probe with an encapsulated active area (containing embedded NWs) generates a huge amount of charge carriers (6.91 nC) in a single pixel line, with characteristic decay time of 500-600 ms (Fig. 5.4). Recorded response is clearly not piezo-electric. Can one use term “piezo-tronic” (phenomena related to the Schottky barrier height change in semiconducting piezoelectrica)? – it should be cleared in the following studies. Long-term electrical response measurements performed during the force magnitude variations at constant bias of 10 V are displayed in Fig. 5.3. Despite of the fact that some qualitative information on the signal magnitude increase can be seen in the time-domain, no quantitative information has been derived due to the signal magnitude instability and high noise level.

Summarizing, PoC2 chips fabricated on sapphire substrates delivers much better signal comparing with PoC2 on silicon in terms of quality and electro-mechanical stability. However, the electrical and mechanical “fragilities” of NWs in both cases do not allow for the higher mechanical or electrical load to be applied in order to get record more clear signal for force-gradation measurements. The main hinder for the multi-channel measurements is a non-equality of the NW properties: electrical, mechanical and perhaps, geometrical. The consequence of this property difference is that for each pixel the load force (set point and amplitude) should be adjusted individually in order to get the recordable signal with no mechanical damages of the NW structure.

5.3 Characterization of encapsulated PoC3 sensors

The principal features and technical layout of PoC Option 3 sensor are described in the Sections 2.2-2.4 of this report. Three types of top contacts have been tested during the experiments on prepared (encapsulated & plasma etched) sensors (2 samples per one type):

- **Type 1**: 100 nm thick evaporated gold top electrode (P03-24);

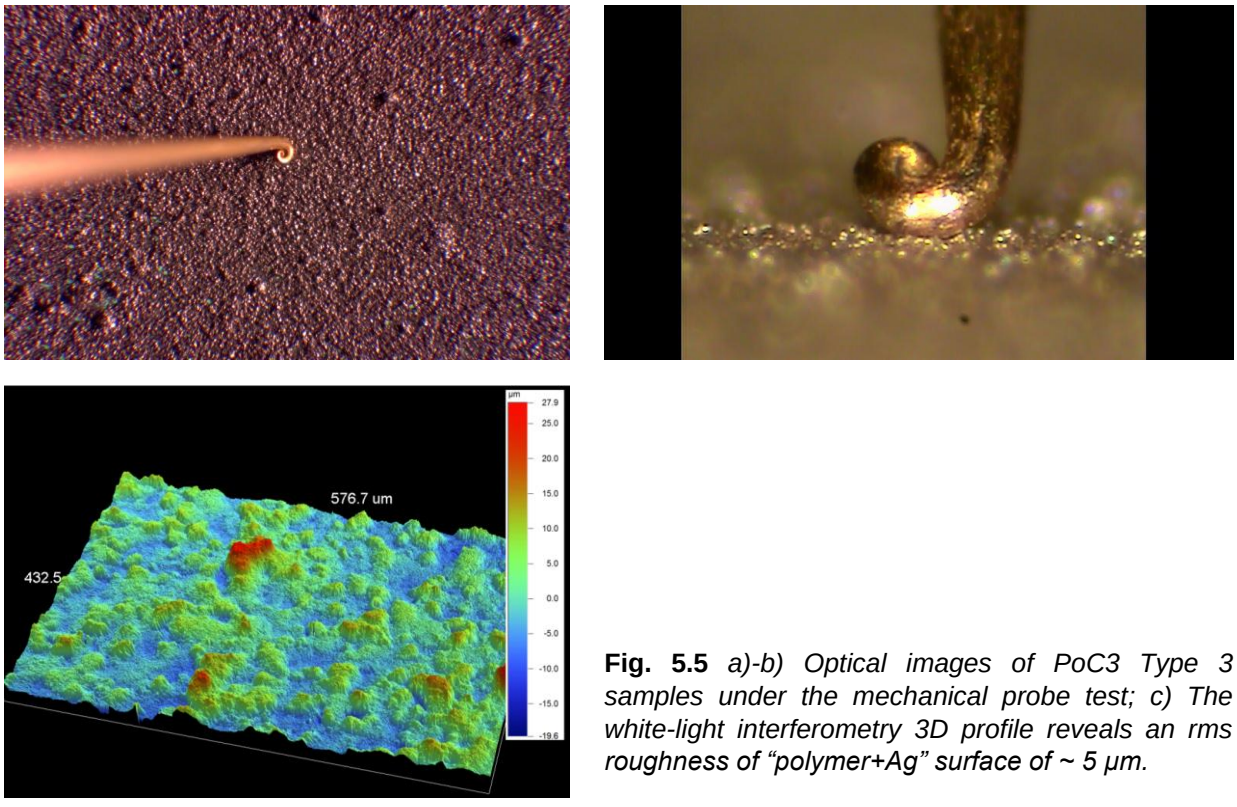

Fig. 5.5 *a)-b) Optical images of PoC3 Type 3 samples under the mechanical probe test; c) The white-light interferometry 3D profile reveals an rms roughness of “polymer+Ag” surface of ~ 5 μm.*

- **Type 2**: thick top contact consisting of pure Ag nano-particles (P07-2);
- **Type 3**: hybrid, Ag-doped polymer layer (P07-7);

For the piezo-electrical tests of encapsulated PoC3 samples, the “macro-probe” measurement environment has been employed, similar to PoC2 characterization. In the majority of the experiments, the top-electrode has been grounded having the same electrical potential as the tungsten mechanical probe. The positive and negative potential has been supplied to the bottom electrode of each NW pixel individually. The read-out has been realized via recording in situ changes in the electrical current vs. time plot. Electrical current vs. time curves have been recorded simultaneously for 4 channels (pixels) using programmed Keithley 2611A source-meters in a high-resistance 4-wire configuration.

In the current report, the results obtained on **type 3** samples are mostly described due to the lower feasibility of the **types 1 & 2** detected during the macro-probing tests. The drawbacks of **Type 1** with thin Au electrodes have been considered in Section 2.4. Besides the observed cracks in the Au layer, there is another obstacle preventing its use for the functional sensor devices – combination of thin polymer matrix and ultra-thin metal electrode does not protect fragile NW pixels sufficiently from the macro-probe impact. Similar to the AFM-tip experiments, the NWs cannot sustain a high force load, while limiting the force magnitude to the 10 µN results in the low-level signal lying within the noise-band. Such signal can be extracted only by a post-measurement Fourier analyses, and

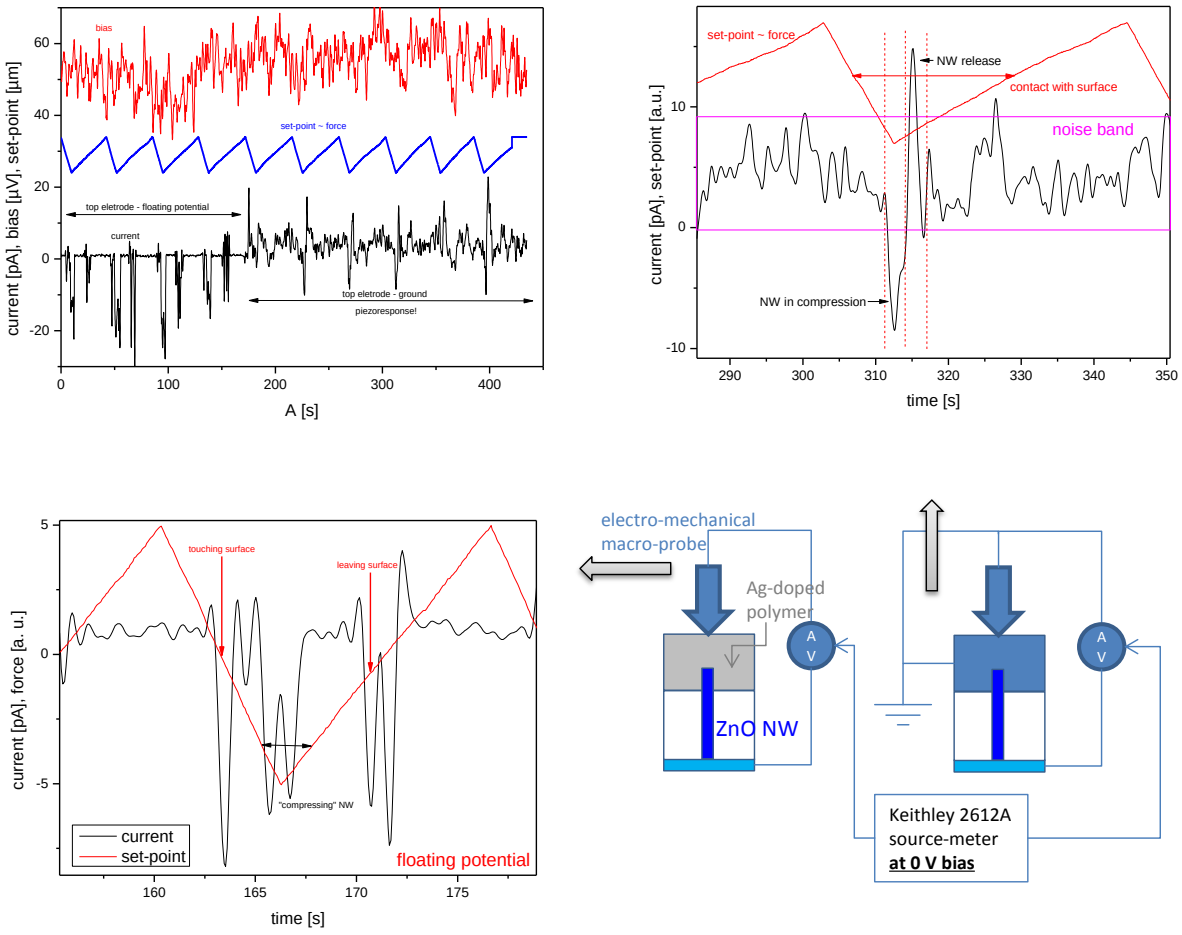

Fig. 5.5 *(top-left) Electrical response of PoC3 Type 3 sample on a periodical force impact of ~ 10 mN in magnitude applied via profiled mechanical probe. The measurements were carried out in two regimes differentiating by top electrode potential, which was either floating (left-bottom) or grounded (right-top).*

is difficult to be used in practice.

On the other hand, the **Type 2** samples deliver a well-defined electrical response. However, due to the thickness of Ag-nano-particle top-electrode, which cannot be accurately controlled on µm level, the acting force from profiled mechanical probe is averaged over the whole NW matrix. In this case, all functioning pixels detect comparable level of electrical signal with no required lateral resolution.

The main results, described in this report have been obtained on the samples of **Type 3** protected by combination of an insulting polymer matrix and a composite "polymer + Ag" top-electrode (Fig. 5.5). All tests have been performed in "no-bias" conditions. Comparing to the **Type 1**, a thicker conducting polymer electrode means also a drastically improved protection of NWs from rough mechanical impact of the prober. On the other hand, the thickness of the polymer can be controlled quite precisely on µm level guaranteeing the individual mechanical impact (low cross-talk) onto each NW pixel within the array.

Two drawbacks are characteristic for **Type 3** technology. First, the NW active area, which is truly embedded in the opaque polymer matrix, is difficult for probe positioning. Second, a high surface roughness of polymer electrode is a serious challenge, and should be optimized to achieve a high lateral resolution of the sensor. Nevertheless, the results obtained on **Type 3** samples are encouraging enough to accept this configuration as a main route for the DEMO chip technology.

As shown in the diagram presented in Fig. 5.5, the electrical response of PoC3 **Type 3** sample on a periodical force impact is well-defined with the acting force magnitude up to 10 mN. The measurements were carried out in two electrical configurations. First, "the top electrode at a floating potential" was used to record the time/position of the prober touching and leaving the sensor surface by detecting specific distortion peaks in the current level (see the "left-bottom" graph). The grounded top-electrode configuration (the "right-top" graph) allows recording of an electrical response related to the direct reaction of the pixel on the mechanical force explicitly. It appears when the force magnitude is reached the level required to deform the NWs within the matrix to the degree essential for the detectable level of the generated current (probe-down). The revers process with the current peak of the opposite polarity is detected, when NWs restoring the initial form following the reduction of the pressure (probe-up). This behavior has been also observed on the single-crystalline ZnO NWs (sapphire substrate) under AFM-tip probing. This data can be found e.g. in the **2nd Annual Report.** on the PiezoMAT web site.

The generated charge per multi-NW pixel, Q_{px}, measured on encapsulated PoC3 samples **Type 3** is in pC range. As derived from Fig. 5.5 plot using simple integration of the current-response peak over time, $<|Q_{px}|>$ ranging from 13.2 to 19.1 pC is typically obtained. Statistical analyses have been carried out on 24 independent channels of the sample Po7-7. Despite of the variations in geometry of the individual "multi-NW" pixels (see Fig. 2.2), the results are reproducible indicating homogeneous conditions for GZO seed spot processing along with optimized growth conditions for the ZnO NW growth at every nucleation spot over the whole active area surface.

5.4 Force-calibrated measurements of encapsulated PoC3 sensors

The sensitivity of the force sensor (S2M-10N) does not allow to make the force measurements in situ, mostly due to the impact of bulky and heavy signal cables and/or needle probers. Therefore, the absolute force calibration has been carried

out in the same geometrical configuration but with the PoC3 PCB not electrically connected by any means. The consolidated results from calibration procedures and from time-domain measurements all are shown in Fig. 5.6.

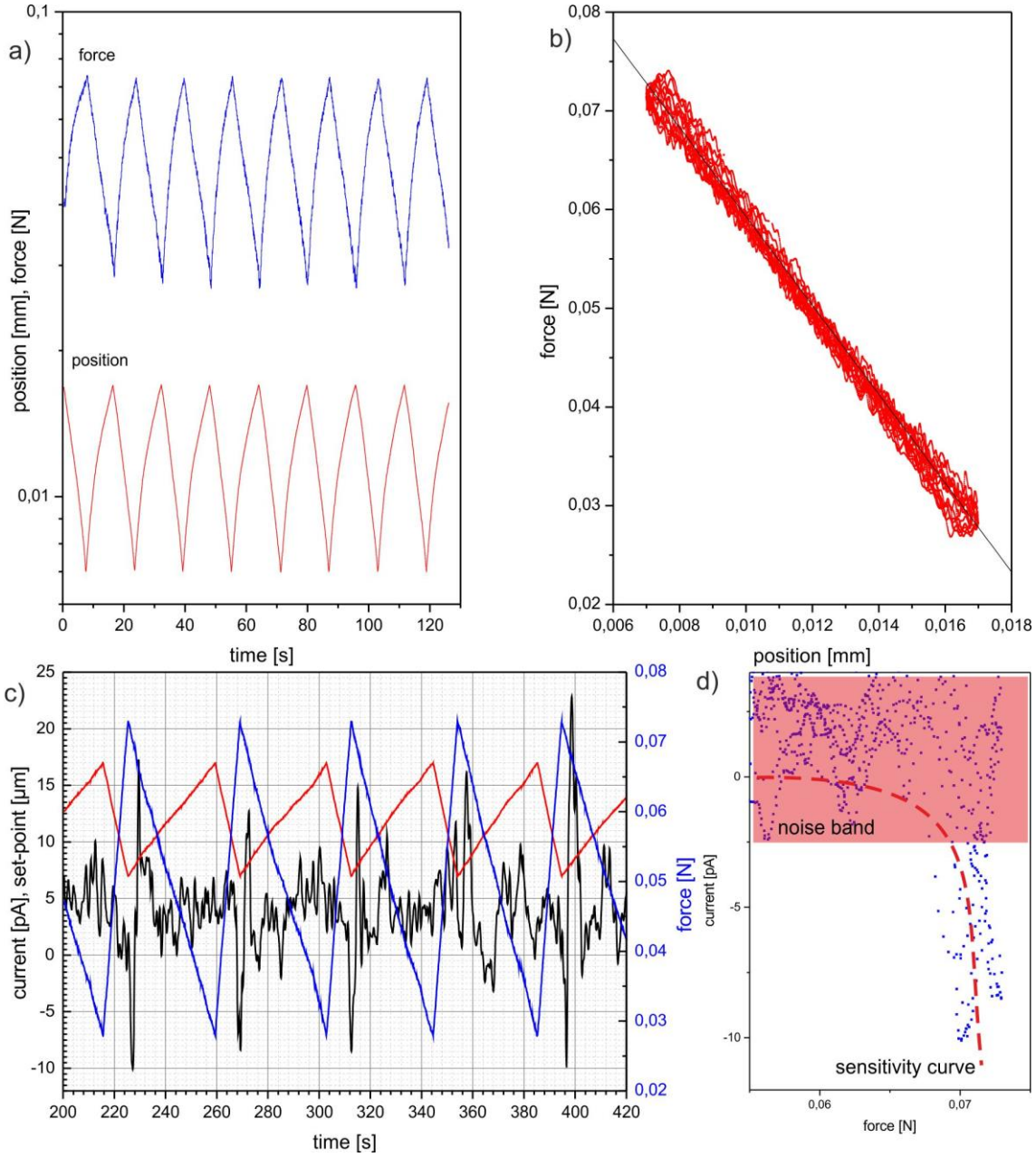

Fig. 5.6 *Calibrated force measurements of piezo-response on PoC3 sample: a) time-domain record of the force-sensor and nano-positioning unit data; b) calibration curve for the applied force as a function of the z-position; c) PoC3 pixel response with calibrated force data on the time-scale; d) the sensitive curve derived from in situ electrical response and calibration data.*

For the calibration procedure, first, the time-domain measurements of z-position (from nano-positioning unit) versus applied force (from force sensor controller) have been performed at 200 Hz repetition rate and then analyzed (Fig. 5.6). As it can be seen in Fig 5.6b, the force response is in a linear regime for the z-position range chosen for the measurements. Please note that force load level of 100 mN

is already critical for the consistency of the NW pixel. To prevent the plastic deformation of the NWs, the measurements have been performed in the "safe" regime up to 75 mN level of the applied forces. In the Fig. 5.6d, the derived sensitivity curve for the PoC3 channel is depicted. In the "linear" work region ranging from 65 to 75 mN, the absolute sensitivity of the sensor is of ~3.1 nA/N.

5.5 Discussion: role of the piezotronic effect

The derived values of generated charges per PoC3 multi-NW pixel exceed the values obtained on stand-alone, single crystalline ZnO NWs by ~3 orders of magnitude. The NWs grown on AZO/sapphire substrates demonstrated the generated charge per NW of Q_{NW} ~ 50 fC at 200 nN applied force (see the deliverable D3.2 and the 1st Annual report). Analytical model taking into account spontaneous polarisation charges transferred from NW to a measuring circuit after physical contact of conducting AFM tip to a NW has been suggested by Tyndall in order to explain an unexpectedly high level of generated charge derived from the experiments. As the top contact uniting PoC3 NWs and the mechanical probe are both grounded, such consideration cannot be used to explain the electrical response obtained on PoC3 samples, because the NW pixel remains in the contact with the measurement circuit permanently.

Three factors have been taken into the account for the following discussion:

1) the magnitude of applied forces was extended to 10-100 mN range in "macro-force" studies of encapsulated sensors;
2) the PoC3 pixel has multi-NW structure with up to 100 parallel-connected NWs, which electro-mechanical actions are nearly independent from each other;
3) ZnO has both, the piezoelectric and semiconducting properties, being a **piezotronic material**.

Obviously, each of these three factors contributes to the observed enhancement in the response signal of the NW force sensor. However, accurate estimation of the individual contribution of each factor to the response is a long-term task. Very roughly, the expected generated charge due to the pure piezoelectric effect in a single NW within 0.2 - 1 µN force range is of 10-100 electrons (10^{-18}±10^{-17} C). In an no-loss case, the increase in applied force magnitude and NW number per pixel by factor of 1000 and by factor of 100, respectively, gives the maximal enhancement factor for the generated charge of ~10^5. The resulting estimated maximal generated charge is still in the range from 0.1 to 1 pC – much lower than

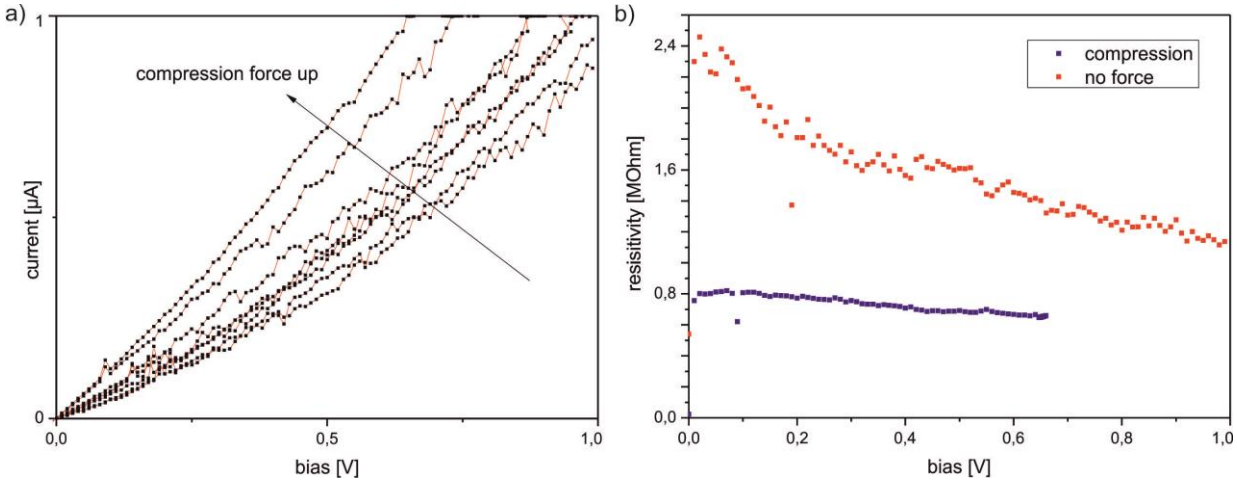

Fig. 5.7 *The results of current-voltage measurements of PoC3 multi-NW pixel under variable compressive force conditions: a) the I-U curves, and (b) the resistance as a function of applied bias taken at two boundary cases – no-pressure (in contact) and high compressive load represented by the red and blue curves, respectively.*

the experimentally obtained response signal from ZnO NW pixel. It requires an introduction of additional current enhancement mechanism, characteristic for piezoelectric/semiconducting ZnO NWs - *the piezotronic effect*. The piezotronics combines phenomenon of piezoelectric polarization with semiconductor properties and allows the direct and active interaction between devices and mechanical stimuli.[2] With a high probability, it is a decisive part of the ZnO NW sensor model, which allows fitting the experimental data obtained on stand-alone NW, PoC2 and PoC3 samples.

The coupling between the piezoelectric and semiconducting properties of NWs was discovered in 2006,[3] in which the strain-induced piezoelectric polarization was used to tune the conductivity of the ZnO NW. This effect was called *the piezotronic effect*, and has been investigated in piezoelectric, semiconducting nanomaterials like ZnO, ZnS, CdS, InN, GaN, etc. The piezotronic effect exists in heterojunction systems with one material being a piezoelectric semiconductor and the other being conductor or semiconductor; e.g. n-ZnO NWs along with Ag-doped polymer and Au bottom contacts in our particular case. When ZnO NW is deformed, polarization charges are induced at both ZnO/metal junctions, which modify the interfacial band structure and thus the carrier transport, trapping, generation, and recombination processes.

[2] Kory Jenkins, Vu Nguyen, Ren Zhu, Rusen Yang, Piezotronic Effect: An Emerging Mechanism for Sensing Applications, Sensors 15, 2015 (p. 22914)

[3] Wang, X.D.; Zhou, J.; Song, J.H.; Liu, J.; Xu, N.S.; Wang, Z.L. Piezoelectric field effect transistor and nanoforce sensor based on a single ZnO nanowire. *Nano Lett.* **2006**, *6*, 2768–2772.

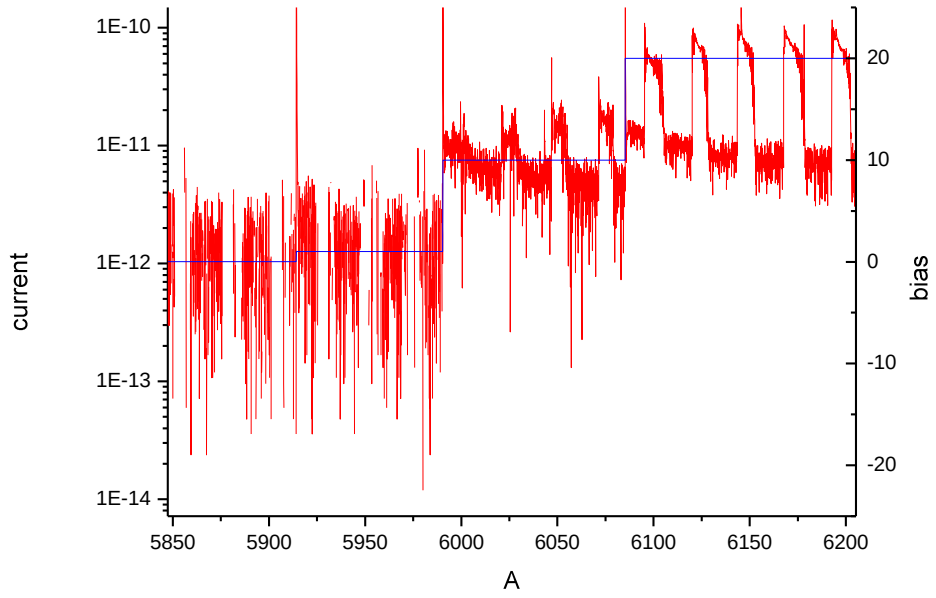

Fig. 5.8 *The generated current under cyclic compressive load recorded on PoC3 pixel at different applied biases (0-20 V, time-domain).*

In our case, ZnO forms Schottky rectifying contact with high work function electrodes: silver (ϕ = 4.26 eV) on top and gold (ϕ = 5.1 eV) at the bottom. It allows only electron transport from ZnO to metal preventing the electron transport from metal to ZnO. Two back-to-back Schottky diodes result in a very limited current flow at the equilibrium conditions. Under strain, however, the polarization charges appear on the opposite ends of the NW, which are partially compensated by internal and external free carriers, but may not completely diminish due to the moderate doping level and finite charge screening lengths of electrodes. At steady state, remnant piezoelectric charges still exist at the two contacts, and the electrostatic field from those positive charges reduces the Schottky barrier height, while negative charges raise the Schottky barrier height. The asymmetric barrier change makes it easier for electrons to transport in one direction. As shown in Fig. 5.7, this effect has been directly confirmed on PoC3 chips by measuring the NW resistivity (via recording *I-U* curves) at different compressive strain conditions induced in ZnO NW via mechanical prober of the "macro-force" setup. The straightforward interpretation of the obtained results is quite difficult due to the demonstrated multi-NW nature of the PoC3 pixel. However, the observed change in the resistivity of the NW under compressive load is indicative for the expected piezotronic effect

In addition, the analyses of the dynamic response carried out on PoC3 NW pixels, can provide an extra indication of the piezotronic behaviour of the electrical signal. As shown in Fig. 5.8, the response signal level along with SNR is significantly improved at 20 V applied bias comparing to the "zero" volt measurements. This data, however, needs an additional experimental confirmation to be conducted with other types of PoC3 samples. The response dynamic parameters fit also a "non-transient" character of the piezotronic effect. In a defect-free system, as long as the strain holds, remnant piezoelectric charges can stay at the interface and the piezotronic effect will not disappear. In

the real devices, decay in current over time is observed due to e.g. recombination and trapping of the charge carriers.[4]

Currently the enhanced FEM model (COMSOL) is being developed at KTU (WP3), which includes a contribution of the piezotronic effect into the calculations of the consolidated electrical response of the PoC3 pixel embedded into the polymer matrix. Preliminary results demonstrate that the current level in pA range is achievable at force range up to 100 mN.

6 NW bending tests at MTA EK MFA

NW bending tests were carried out on both as-grown and encapsulated PoC2 samples (Fig. 6.1).

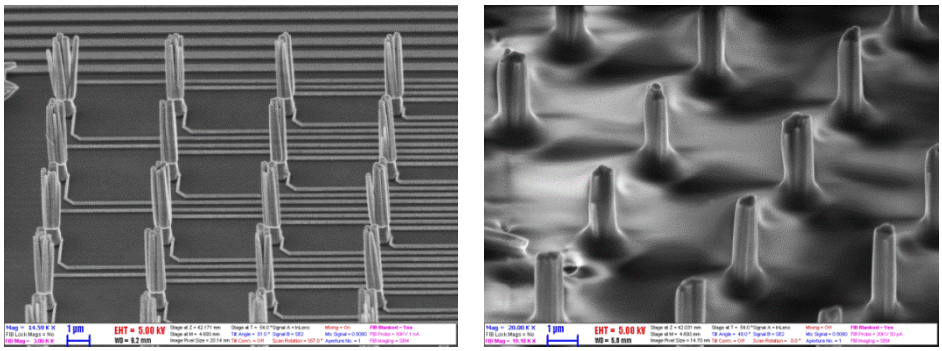

Fig. 6.1 *PoC2 Si chip (W3356_19) before (a) and after (b) polymer encapsulation.*

The contacted NWs had non-liner I-V curves. Upon NW deflection some of them showed significant change in their I-V characteristics (Fig. 6.2). The signal was reproducible in several loading cycles. It was also found that the experiment is more reproducible on polymer encapsulated samples. Moreover, they showed much higher fracture strength compared to as-grown NWs.

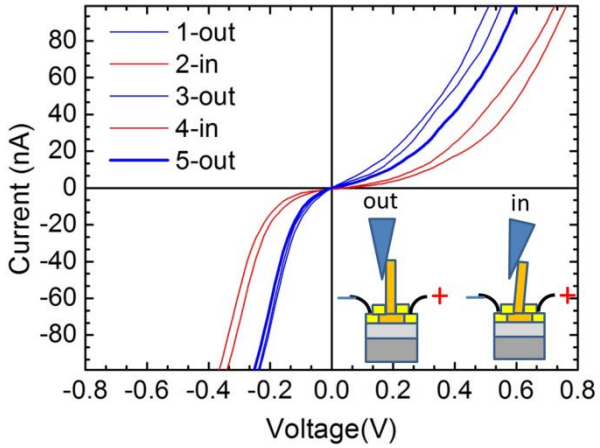

Fig. 6.2 *Current-voltage curves taken at subsequent loading cycles. The unloaded and loaded curves are fairly reproducible.*

[4] Zhou, J.; Gu, Y.; Fei, P.; Mai, W.; Gao, Y.; Yang, R.; Bao, G.; Wang, Z.L. Flexible piezotronic strain sensor. Nano Lett. 2008, 8, 3035–3040.

Time-domain measurements revealed very high bending sensitivity and fast response time. In the experiment shown in Fig. 6.3a for instance a 20% change in the current was found at a cyclic lateral loading force of 2 uN and a bias voltage of -0.2V. In the next experiment a box-car type loading profile was followed by up- and down-staircases which resulted in down- and up-ramps in the current at a bias voltage of 0.5 V.

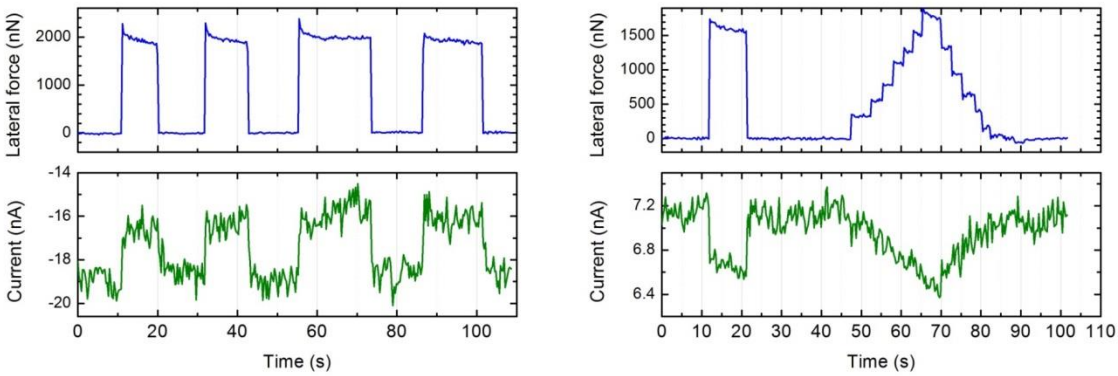

Fig. 6.3 *Time-domain NW bending tests on two different NW taxels of a PoC2 chip (W3356_19) at bias voltages of -0.2V (a) and 0.5 V (b). Current signals follow the lateral loading profiles.*

In summary some of the NWs showed high sensitivity on NW tip deflection. Encapsulated NWs have higher fracture strength and provide more clear signals. A systematic investigation is currently in progress to elucidate the effect of polymer encapsulation and NW geometry on the obtained electrical signal.

7 Summary of D6.3.x

The deliverable D6.3.x is a compilation of experimental work carried out in work package 6 comprising the results obtained in “T6.3: Testing of PoC NW matrix prior to encapsulation” and “Task T6.4: Testing of PoC NW matrix following encapsulation”.

Summarizing the current results in the field of piezo-electro-mechanical characterization of force sensors based on PoC2 and PoC3 concepts, the following technical achievements should be highlighted:

1. all equipment constituents required for the precise electro-mechanical characterization of ZnO NW-based pixels have been developed, constructed and approved at Fraunhofer (measurement setups, PCBs, analog and digital interfaces, data acquisition systems, etc.);
2. within the reported period over 10 fully processed sensor chips of Option 2 & 3 have been fabricated by PiezoMAT partners and characterized in T6.3 and T6.4;
3. high feasibility in fabrication of the POC 2&3 sensors has been demonstrated by the consortium; it includes many comprehensive technological steps such as clean-room processing of the patterned carrier chips (CEA) followed by selective growth of ZnO NWs (MTA and ULEI) and NW encapsulation into polymer matrix (SP) finalized by top electrode fabrication for PoC3 version (MTA, SP, Fraunhofer).

The results of experimental studies carried out on PoC2 and PoC3 sensors can be briefly summarized in the following way:

4. electro-mechanical characterization of not encapsulated PoC2 & PoC3 sensors using AFM-based techniques did not deliver expected results due to the high fragility of the free standing NW pixels, which cannot sustain any lateral force load. The reachable magnitude of the applied compressive force (z-axis) of ~ 100 nN has not allowed recording reproducible piezo-electrical response. The optimization of NW growth targeting a structurally improved GZO/NW interface is under way at MTA;
5. force-dependent sensor response has been detected on both encapsulated PoC2 and PoC3 multi-channel samples (proof-of-concept); the force dependence, however, cannot be precisely quantified at the moment due to the significant signal drift and electro-mechanical instability of the pixel NWs under long-term cyclic mechanical load; the measurements of PoC samples with improved structural properties of NWs are planned for the further studies;
6. the decisive role of the piezotronic effect has been confirmed by analyzing static and dynamic electrical characteristics of the NWs by varying mechanical load (strain) and bias conditions; this topic is of high importance for the future PiezoMAT development, as from the technical (DEMO chip fabrication) as from the scientific (theoretical modelling and publications) points of views.

The fabricated, high-quality PoC samples of both modifications are advanced sensor devices. Therefore, in-depth studies of their properties bring important scientific information helping to understand many phenomena occurring in piezotronic nano-systems. The studies of PoC2 & PoC3 sensors are constantly in progress and will be continued by PiezoMAT consortium in the future, i.e. to support the activities towards DEMO chip development, fabrication and characterization.